Laser and Particle Beams (2007), *25*, 267–275. Printed in the USA.

DOI: 10.1017/S0263034607000110

X-ray spectroscopy observation of fast ions generation in plasma produced by short low-contrast laser pulse irradiation of solid targets

A.YA. FAENOV,[1] A.I. MAGUNOV,[2] T.A. PIKUZ,[1] I. YU. SKOBELEV,[1] S.V. GASILOV,[1] S. STAGIRA,[3] F. CALEGARI,[3] M. NISOLI,[3] S. DE SILVESTRI,[3] L. POLETTO,[4] P. VILLORESI,[4] AND A.A. ANDREEV[5]

[1]Joint Institute for High Temperatures of Russian Academy of Sciences, Moscow, Russia
[2]A.M. Prokhorov General Physics Institute of Russian Academy of Sciences, Moscow, Russia
[3]National Laboratory for Ultrafast and Ultraintense Optical Science - CNR - INFM, Department of Physics, Politecnico, Milano, Italy
[4]Laboratory for Ultraviolet and X-Ray Optical Research - CNR - INFM, D.E.I. - Universita di Padova, Padova, Italy
[5]Institute for Laser Physics, S.I. Vavilov State Optical Institute, St.-Petersburg, Russia

(RECEIVED 28 November 2006; ACCEPTED 15 January 2007)

Abstract

X-ray spectra of plasma produced by the interaction of Ti:Sa laser pulses (duration from 60 fs to 1 ps, and energy from 15 mJ to 128 mJ) with foil and solid Teflon and AL targets are investigated. It is shown experimentally and theoretically that the use of low contrast ($10^{-2} - 10^{-4}$) short laser pulses, essentially promotes the conditions for generation of fast multi-charged ions. This effect is caused by self-focusing of the main laser pulse in a preplasma produced by intense laser prepulses. Modeling of the observed spectral line shape gives evidence of a considerable (about 3%) amount of multi-charged He-like F ions with energy $E \sim 1$ MeV at rather low values of laser intensity $I_L \approx 6 \times 10^{16}$ W cm^{-2}.

Keywords: Ion acceleration; Laser beam self-focusing; Laser-produced plasma; X-ray spectroscopy

1. INTRODUCTION

Intense laser pulses, interacting with matter, create plasmas with nonequilibrium energy distribution of electrons and ions. Creation of high-energy ions in an amount that noticeably exceeds the values followed from the equilibrium distribution function is usually mentioned as fast particles generation in plasma. Investigation of ion acceleration mechanisms allows the realization of highly effective laser-plasma accelerators of protons, electrons, and heavy ions (Mourou *et al.*, 2006; Lifshitz, 2006; Mangles *et al.*, 2006).

Generation of fast particles in plasma by nanosecond laser pulses has been experimentally studied for several decades (Gitomer *et al.*, 1986). Empirical scaling laws describing the dependence of fast ion energy from the parameter $F = I_L\lambda_L^2$, which is associated with the laser wavelength and laser intensity, have been obtained, where I_L is the laser radiation intensity, and λ_L is the wavelength. With flat solid-state targets and nanosecond laser pulses, fast ions of 1-MeV energy were observed at $F \sim 10^{13}$–10^{14} W/cm^{-2}/μm^2 (Rosmej *et al.*, 2002; Schaumann *et al.*, 2005).

For pico- and subpicosecond pulses, the condition for fast particle generation worsens, and an appreciable quantity of fast protons and multi-charged ions are observed only at essentially higher values of $F > 10^{18}$ W/cm^{-2}/μm^2 (Key *et al.*, 1998; Dobosz *et al.*, 1999; Zhidkov *et al.*, 1999, 2001; Krushelnick *et al.*, 2000; Maksimchuk *et al.*, 2000, 2004; Auguste *et al.*, 2001; Andreev *et al.*, 2002; Magunov *et al.*, 2003; Fukuda *et al.*, 2004; Belyaev *et al.*, 2004, 2005; Cowan *et al.*, 2004; Fuchs *et al.*, 2005; Lindau *et al.*, 2005; Fernandez *et al.*, 2005; Brambrink *et al.*, 2006*a*, 2006*b*; Hegelich *et al.*, 2006; Yin *et al.*, 2006). Besides high intensity of laser radiation, experiments described in these papers were conducted at rather high pulse contrast, and accordingly, at small-scale heterogeneity of plasma density (Laska *et al.*, 2006).

Usually, the focused radiation intensity in a vacuum is used to estimate the value of the F parameter. However, the actual local F parameter value in plasma can be essentially higher, e.g., in the presence of laser beam self-focusing

Address correspondence and reprint requests to: Anatoly Ya. Faenov, Joint Institute for High Temperatures of Russian Academy of Sciences, Izhorskaja str. 13/19, 127412 Moscow, Russia. Email: anatolyf@hotmail.com

(SF). Thus, if there is a SF of laser radiation in plasma, conditions for the fast particles generation defined by F parameter are considerably softened. Indeed, fast ions can be observed at much smaller F-values. Such an effect was observed recently in Kim *et al.* (2006), where 1-MeV H-like oxygen ions have been observed at SF of femtosecond pulses in a cluster targets at values of $F \sim 10^{16}$–10^{17} W/cm^{-2}/μm^2.

In this paper, it is experimentally shown, that a similar effect takes place in solid-state targets heated up by femto- and picosecond pulses of low contrast. In this case, the SF of the main laser pulse occurs in rather long preplasma, created by a laser prepulse. In such conditions, the appreciable quantity of multi-charged ions with energy $E \sim 1$ MeV is generated at values of $F \sim 10^{16}$ W/cm^{-2}/μm^2 for the main laser pulse.

2. EXPERIMENTAL SETUP

The experiment has been performed using a Ti:Sapphire (Ti:Sa) laser system of national laboratory for ultrafast and ultraintense optical science (ULTRAS-CNR-INFM, Politecnico di Milano, Italy), which generates 800 nm pulses with 10 Hz repetition rate, maximum energy of 130 mJ, and minimum duration of 60 fs. The duration of laser pulses was varied, between 60 fs and 1 ps changing the distance between gratings in the compressor stage. The laser pulse contrast was $\sim 10^{-5}$ in the nanosecond time scale and $\sim 10^{-4}$ in the ps scale.

The scheme of the experimental setup is shown in Figure 1. Teflon slab (CF_2), and CF_2 and Al foils of various thickness were used as targets. The laser beam was focused on a target surface at an incidence angle of 15° by an off-axis parabola mirror in a spot of 10–20 μm in diameter (The Rayleigh length of focusing system in a vacuum is about 200 μm). The peak intensity varies in the range $I_L = 4 \times 10^{15}$–6×10^{17} W/cm^{-2} for the pulse duration from 1 ps to 60 fs. The target was continuously shifted in order to shoot each time on a fresh surface. Laser radiation focusing and plasma expansion were controlled by an X-ray pinhole camera with a 15-μm aperture diameter. The 1:1 plasma image was recorded on a RAR-2492 film in the X-ray spectral range above 0.4 keV photon energy.

In this experiment, we intentionally reduced the laser pulse contrast to about 10^{-2} in the 100-ps scale by inverting a dielectric steering mirror between the regenerative and the high power amplifiers: in this way, a weak prepulse reflected from the substrate surface was generated. Figure 1b presents the pinhole image of the expanding plasma produced by focusing of the laser pulse with energy $E_L = 128$ mJ, and duration $t_L = 1$ ps on the surface of 13-μm Al foil. The intensity traces along and transverse to the laser beam propagation directions are shown in Figure 2. The plasma image and its traces manifest an evidence of the laser radiation channeling due to the SF effects. A noticeable modulation of the X-ray radiation intensity along the plasma region also testifies to

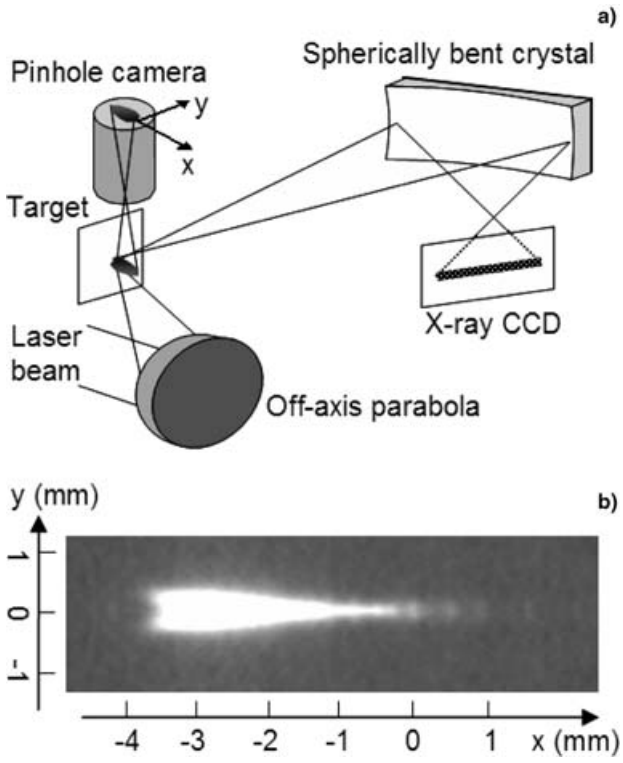

Fig. 1. (**a**) Experimental setup. (**b**) Pinhole X-ray image of plasma produced by irradiation of the 13-μm Al foil target by the Ti:Sa laser pulse of 1 ps duration and 128 mJ energy (the target surface is at $x \approx 0$).

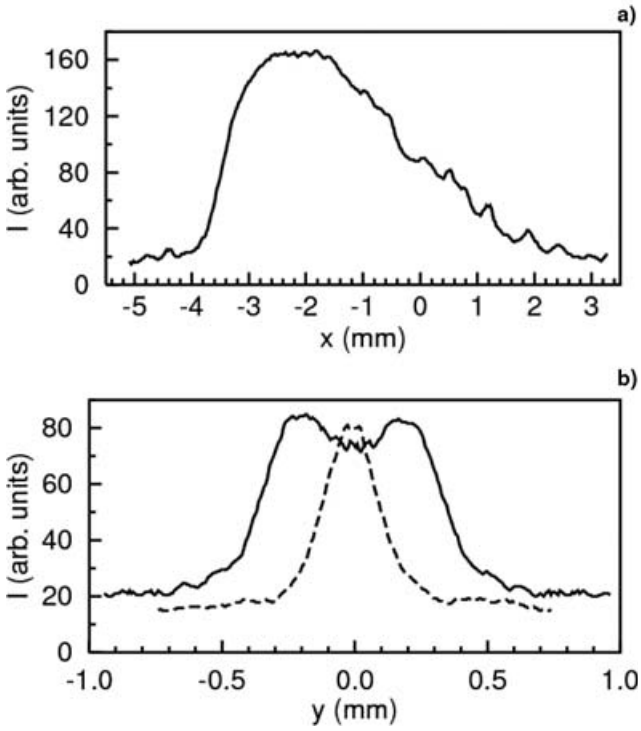

Fig. 2. (**a**) X-ray intensity distribution obtained from the pinhole image in Fig. 1b along the laser beam propagation axis. (**b**) X-ray intensity distribution transverse to the laser beam propagation direction at $x \approx -3.5$ mm (solid curve) and $x \approx 0.5$ mm (dashed curve).

https://doi.org/10.1017/S0263034607000110 Published online by Cambridge University Press

the SF regime of the laser beam propagation in the plasma channel (Bulanov *et al.*, 1995).

X-ray radiation spectra of plasma were measured by the focusing spectrometer with spatial resolution (FSSR) spectrometer (Faenov *et al.*, 1994; Skobelev *et al.*, 1995) based on the spherically bent mica crystal ($2d = 1.991$ nm). The crystal curvature radius is $R = 100$ mm and the aperture size is 8×26 mm^2. The X-ray radiation was registered by the CCD camera (Roper Scientific, 1300×1300-cells matrix) with the cell size of 20 μm. The CCD-matrix was protected from the visible and vacuum ultraviolet VUV radiation by three layers of the 1-μm polypropylene film covered by the 0.2-μm Al layer. The spectrometer was adjusted to the first order Bragg reflection at the angle $\theta_{Br} = 49.8^\circ$ to observe the He$_\beta$ line of He-like ion F-8 ($1s3p - 1s^2$ resonance transition), and the Ly$_\alpha$ line in H-like ion F-9 ($2p - 1s$ resonance transition) with the spectral resolution $\lambda/\Delta\lambda \approx 5000$ in the wavelength range 1.41–1.62 nm. The spectral measurements were performed with the one-dimensional spatial resolution about 50 μm transverse to the plasma expansion direction.

3. FAST IONS DIAGNOSTICS AND MODELING

X-ray spectroscopy diagnostics of fast ions in plasma is based on the fact that the spectral line shape is sensitive to the ion velocity distribution function due to the Doppler effect (Dobosz *et al.*, 1999; Zhidkov *et al.*, 1999; Magunov *et al.*, 2003; Rosmej *et al.*, 2005). Theoretical modeling of the experimentally observed He$_\beta$ and Ly$_\alpha$ line shapes and their relative intensities allows for an estimation of the plasma parameters, namely, the electron temperature and density, and the ion energy distribution function.

Figure 3 presents the experimental X-ray spectra of plasma, produced by 1-ps laser pulses with various energies (15–128 mJ), irradiating the CF_2-slab and the 80 μm foil targets. It is clearly seen that the Ly$_\alpha$-line of F-9 intensity rises sharply with the increasing laser pulse energy. The Ly$_\alpha$ and He$_\beta$ line intensities are nearly equal at the pulse energy of 128 mJ. It means that at higher laser pulse energy and intensity, the H-like ions are formed more effectively in plasma, both due to rising of the electron bulk temperature, and the growth of the hot electron fraction. Figure 3 also shows that the line widths (of He$_\beta$, especially) increase considerably with the laser radiation intensity. Such behavior of the line widths confirms the growth of the accelerated ions fraction. Another feature in Figure 3 is the He$_\beta$ line asymmetry, which appeared at some laser intensities. The long-wavelength ("red") wing of the line is more intense than the short-wavelength ("blue") wing. It is necessary to remember, that the red wings of the resonance lines are usually contributed by the dielectronic satellites; however their intensities in the F ions should be insignificant. More likely, the line asymmetry is due to anisotropy of the fast ion generation in picosecond plasma. Fast ions moving in the laser beam propagation direction (deep into the target) or backward from the direction of observation are more

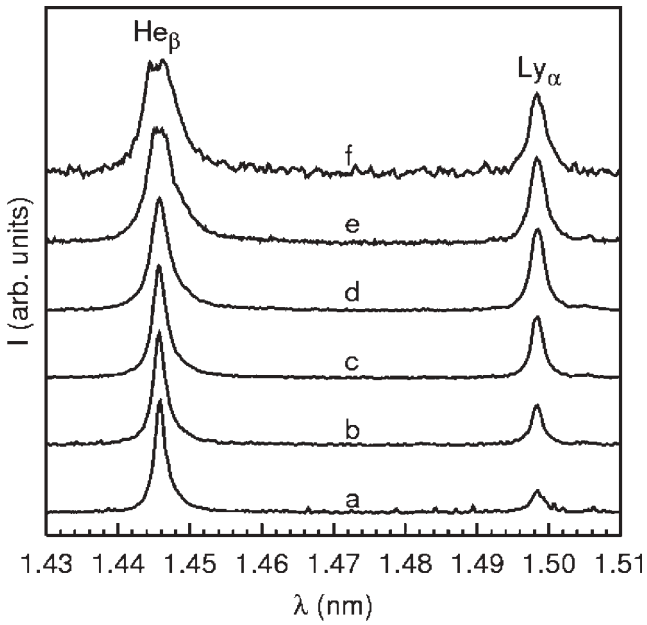

Fig. 3. Measured X-ray spectra in the region of He$_\beta$ and Ly$_\alpha$ lines of F ions in plasma produced by the 1-ps Ti:Sapphire laser pulse irradiating the Teflon slab and the 80-μm foil (at $E_L = 128$ mJ) targets as a function of pulse energy. The curves are normalized to the peak intensity of the He$_\beta$ line. The pulse energy increases for the curves from bottom to top: 15 mJ (**a**), 30 mJ (**b**), 60 mJ (**c**), 120 mJ (**d**), 128 mJ (**e**), for a slab target and 128 mJ (**f**) for a foil target.

effectively produced. Thus, the spectral line shape measurements in our experiments can be used to draw the velocity distribution function of ions in plasma.

Figure 4 shows as an example, the modeling results for the He$_\beta$ (Fig. 4a) and Ly$_\alpha$ (Fig. 4b) line emission of plasma produced by the 120-mJ, 1-ps laser pulse on the CF_2-slab target. The experimental data, shown as symbols, reveal a small asymmetry of the line wings that can be explained by anisotropy of fast ions expansion. In this case, it appears as a bigger laser intensity.

The line intensity for the He$_\beta$ and Ly$_\alpha$ lines in F ions was calculated by the following expression

$$I(\lambda) \propto \lambda^{-1} \sum_j A_j S_j(\lambda - \lambda_j) N_{u,j}, \quad (1)$$

where A_j and λ_j are the radiation transition probability and wavelength of line j, correspondingly, $N_{u,j}$ is the upper level population density for the transition j.

The spectral function $S_j(\lambda - \lambda_j)$ was calculated according to Stark and Doppler broadening because the collisional width is negligibly small at the electron density values about the critical one

$$S_j(\lambda - \lambda_j) = \int W(E) \sum_\alpha \gamma_{j\alpha}(E) f_j \times \left(\lambda - \lambda_j - \Delta\lambda_{j\alpha}(E)\right) dE, \quad (2)$$

https://doi.org/10.1017/S0263034607000110 Published online by Cambridge University Press

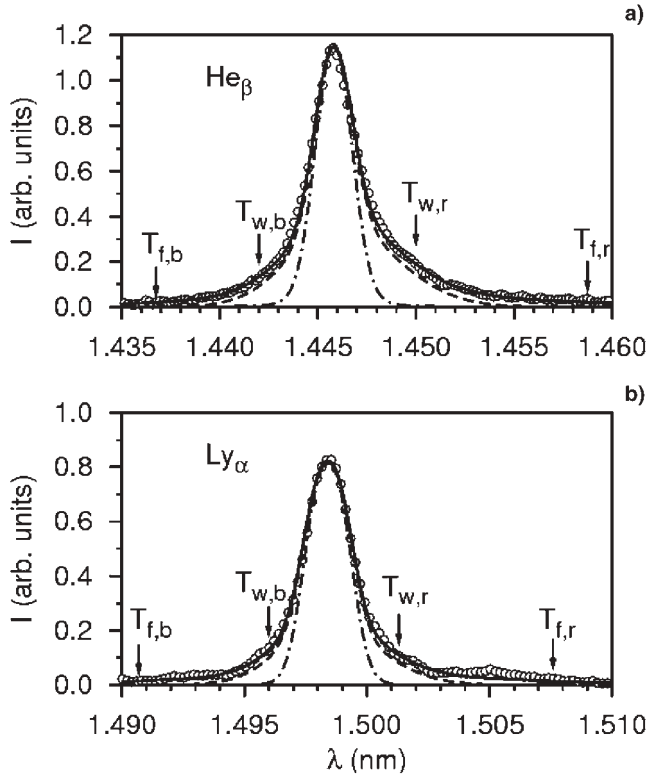

Fig. 4. Spectral line shapes of He_β (**a**) and Ly_α (**b**) lines of F ions in Teflon plasma. The experimental data were obtained with the laser pulse of 1 ps duration and energy 120 mJ (circles). Dash-dotted curves correspond to model calculation of the central part of the line by the integral term in (4) with the following parameters: $N_e = 2 \times 10^{20}$ cm^{-3}, $T_e = 128$ eV, $T_{c,He} = 5$ keV, $T_{c,H} = 4$ keV. Dashed curves show contributions of the second term in (4) to the nearby wings with the parameters: $T_{w,He} = 50$ keV, $T_{w,H} = 25$ keV (blue wings) and $T_{w,He} = 80$ keV, $T_{w,H} = 35$ keV (red wings). Solid curves account for also contributions of fast ions in (4): $T_{f,He} = 0.35$ MeV, $T_{f,H} = 0.25$ MeV (blue wings) and $T_{f,He} = 0.7$ MeV, $T_{f,H} = 0.35$ MeV (red wings). Arrows show the Doppler shift for ions with the energy equal to corresponding temperature values.

where $W(E)$ is the distribution function of the ionic microfield strength E in plasma, $\gamma_{j\alpha}(E) = A_{j\alpha}(E)/A_j$ and $\Delta\lambda_{j\alpha}(E)$ are the transition branching ratio, and the wavelength shift for the Stark component α of the line j, respectively.

The one-dimensional velocity distribution function of ions (velocity projection on the observation direction) $f_j(v)$ was described by the three-temperature dependence in the form

$$f_j(v) = a_{c,j} f_M(\bar{v}_{c,j}, v) + a_{w,j} f_M(\bar{v}_{w,j}, v) + a_{f,j} f_M \times (\bar{v}_{f,j}, v) a_{c,j} + a_{w,j} + a_{f,j} = 1, \quad (3)$$

where $f_M(\bar{v}, v) = 1/(\sqrt{\pi}\,\bar{v}) \exp(-v^2/\bar{v}^2)$ is the Maxwell distribution function defined by the effective ion temperature (in energy units) $T = M\bar{v}^2/2$, M is the ion mass. The first term in Eq. (3) defined by the effective temperature $T_{c,j}$ contributes to the central part of a line in Eq. (2). The second term in Eq. (3) is contributing to the nearby line wings are defined by the effective temperature $T_{w,j}$, while the third term characterizes the far wings by the temperature of fast ions $T_{f,j}$. In order to reproduce the observed line asymmetry different values of $T_{w,j}$ and $T_{f,j}$ (as well as $a_{w,j}$ and $a_{f,j}$), were used for the blue and red line wings in the exponential contributions in Eq. (2). The differences of corresponding values characterize anisotropy of the ions velocity distribution functions. Note, the $a_{c,j}$ values also differ for opposite sign of v in order to obey normalization and continuity of the $fj(v)$ function simultaneously.

The integration in Eq. (2) should be performed with the first term on the right-hand side of Eq. (3) because the widths of two others are much greater than the corresponding Stark shift at typical plasma density. Thus, Eq. (1) reads

$$I(\lambda) \propto \lambda^{-1} \sum_j A_j \Big[a_{c,j} \int W(E) \sum_\alpha \gamma_{j\alpha}(E) f_M (\Delta\lambda_{c,j}, \lambda - \lambda_j - \Delta\lambda_{j\alpha}(E)) dE + a_{w,j} f_M (\Delta\lambda_{w,j}, \lambda - \lambda_j) + a_{f,j} f_M (\Delta\lambda_{f,j}, \lambda - \lambda_j) \Big] N_{u,j} \quad (4)$$

where $\Delta\lambda_{c,j} = \lambda_j \sqrt{T_{c,j}/Mc^2}$, $\Delta\lambda_{w,j} = \lambda_j \sqrt{T_{w,j}/Mc^2}$, and $\Delta\lambda_{f,j} = \lambda_j \sqrt{T_{f,j}/Mc^2}$ are the Doppler halfwidths for the central line region, the nearby and far wings of the line j, respectively; c is the speed of light.

The line profile calculations were performed in the linear Stark shift approximation with the microfield distribution function that accounts for the Debay screening and ionic correlations (Tighe & Hooper, 1976). The average electron density value $N_e = 2 \times 10^{20}$cm^{-3} was used. The line shape obtained for the central part of He_β and Ly_α differs a little from the Doppler profile. The observed intensity ratio of the lines is defined mainly by their central areas. It was fitted by varying the electron temperature T_e in the stationary collision-radiating kinetic model calculation and the effective temperature of ion bulk $T_{c,j}$ that defines the line width. The result of the line fitting obtained with Eq. (4) is shown by solid curves in Figures 4a and 4b. The results obtained with the integral in Eq. (4) are shown by dash-dotted curves. Dashed curves show the contribution of the second term in the right-hand side of Eq. (4). A sensitivity of the line shape to the effective ion temperature values is high enough for their reliability within 10–20%. The accuracy is higher for the $T_{w,j}$ values since the background contribution to the nearby line wings is relatively smaller than to the far wings.

Note Eq. (1) is valid only for optically thin plasma. To account for the absorption near the line center, the uniform layer approximation was used in calculations

$$\bar{I}(\lambda \sim \lambda_j) = \frac{I(\lambda_j)}{\tau_j} [1 - \exp(-\tau_j I(\lambda)/I(\lambda_j))], \quad (5)$$

where τ_j is the line center optical depth of the plasma.

The experimental data at different values of laser pulse parameters were fitted in a similar way. The analysis of

https://doi.org/10.1017/S0263034607000110 Published online by Cambridge University Press

experimental data shows that the distribution function of ions strongly differs from the single-temperature Maxwellian one. The main fraction of the accelerated ions, moving from a target aside spectrometer, is characterized by effective temperatures $T_{w,j} = 30-60$ keV, whereas for ions, moving in the opposite direction $T_{w,j} = 40-80$ keV. Fast ions, moving from a target surface, are characterized by effective temperatures $T_{f,j} = 200-400$ keV, and fast ions, moving in the direction to the target $T_{f,j} = 300-800$ keV.

Figure 5 shows the variation of the ion velocity distribution function (Eq. 3) at fixed laser pulse duration $t_L =$ 1 ps with the laser beam energy and focusing (parameter F). Positive ion velocity corresponds to their motion toward the target surface. The results show that the positive velocity fast He-like ions (Fig. 5a) and H-like ions (Fig. 5b) fractions increase more rapidly with the laser pulse intensity than those with negative velocity.

Figure 6 presents the same characteristics for different pulse duration at fixed energy value $E_L = 120$ mJ. The fast ions fraction sharply declines at 60-fs pulse duration.

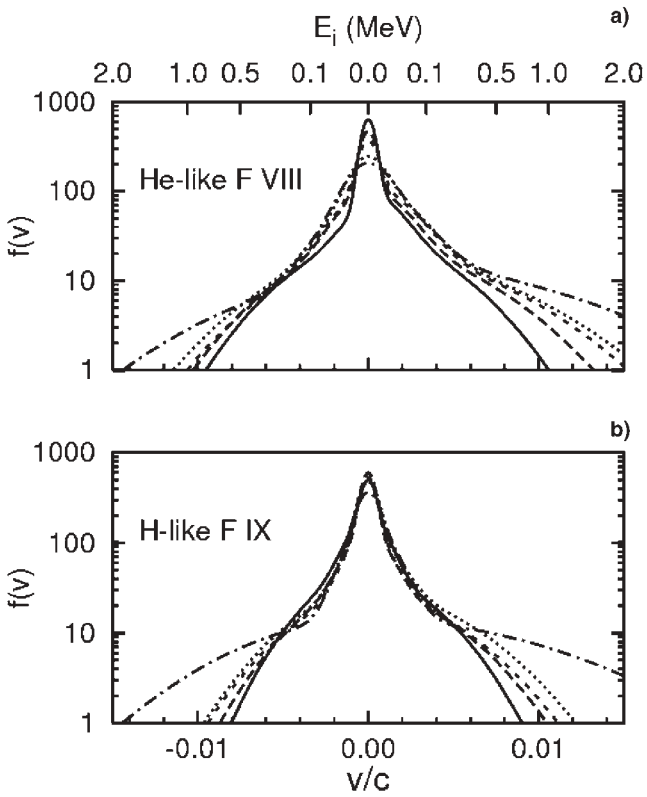

Fig. 5. One-dimensional velocity distribution functions of He-like (**a**) and H-like (**b**) F ions obtained by fitting of (4) to the measured He_β and Ly_α line profiles (see Fig. 3) at fixed pulse duration $t_L = 1$ ps and different laser pulse energies: 15 mJ (solid curve), 60 mJ (dashed curve), 120 mJ (short dashed curve), 128 mJ with slab (dotted curve) and foil (dash-dotted curve) targets. The positive velocity corresponds to the direction of laser beam propagation.

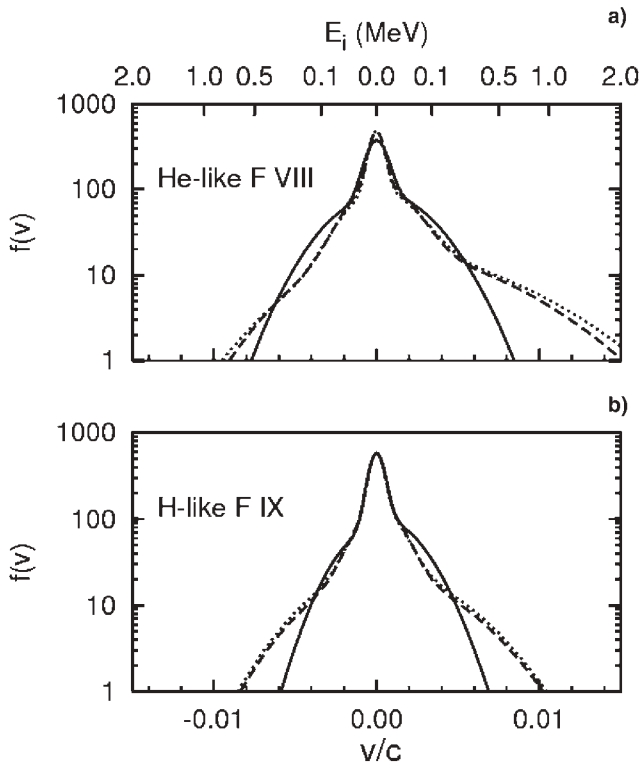

Fig. 6. One-dimensional velocity distribution function of He-like (**a**) and H-like (**b**) F ions obtained by fitting of (4) to the He_β and Ly_α line profiles at fixed energy $E_L = 120$ mJ and different laser pulse durations: 60 fs (solid curve), 600 fs (dashed curve) and 1 ps (dotted curve). The positive velocity corresponds to the direction of laser beam propagation.

The fast ion fraction with energy above E is defined according to Eq. (3) by the integral

$$P_j(E) = b_j \int_{\sqrt{2E/M}}^{\infty} f_m(v_{f,j}, v)\, dv = b_j \times \left[1 - \mathrm{erf}\left(\sqrt{E/T_{f,j}}\right)\right], \quad (6)$$

where erf(x) is the error function. The fast ion fraction followed from our calculations is significant enough. For example, at $F = 4 \times 10^{16}$ W/cm$^{-2}\mu$m^2 (laser beam energy 128 mJ and pulse duration 1 ps) the value of P_j for the He-like ions with energies above 1 MeV is about 3%.

The generation of fast ions can by explained as follows. The non-uniform plasma is created in front of the target during the interaction with an intense laser pulse. The electron density varies from the solid-state value to zero. The scale of the density gradient can be estimated as $L_n \approx c_s t_p$. Here $c_s = (ZT_{e,p}/M)^{1/2}$ is the speed of ionic sound, t_p is the characteristic prepulse duration, $T_{e,p}$ is the electron temperature of preplasma, and Z is the ion charge. In our experiments, the prepulse was significant during more than 100 ps time interval when the pulse contrast reached values of

https://doi.org/10.1017/S0263034607000110 Published online by Cambridge University Press

10^{-2}–10^{-4}. Thus, for laser intensity around 5×10^{16} Wcm^{-2}, the prepulse intensity has the value of 5×10^{12}–5×10^{14} Wcm^{-2}. For simplicity, the plasma corona can be approximated in this case by a homogeneous medium of 100 μm in length with the density $N_e \approx 0.1N_c$. It is worth noting that the critical density for the Ti:Sa laser radiation is $N_c = 1.7 \times 10^{21}$ cm^{-3}.

It is well-known that in such a plasma, the laser beam is subjected to SF if the pulse power P_L (in Watts) is high enough (Sun *et al.*, 1987) to hold inequalities

$$v_E R_L > c\lambda_p, \quad P_L > 3 \times 10^{10} N_c/N_e. \tag{7}$$

Here v_E is the electron oscillatory velocity, λ_p is the plasma wavelength, R_L is the laser beam radius. The laser pulse energy $E_L = 120$ mJ and duration $t_L = 0.6$ ps correspond to conditions near the SF threshold that is overcome at smaller durations. Actually, the plasma is non-uniform, and somewhere, there always exists an area that obeys the SF conditions (Eq. (7)). The length of SF can be estimated by the formula from Kodama *et al.* (1996)

$$L_{SF} \approx R_L \sqrt{\frac{N_c T_{e,keV}}{N_e I_{L,16} \lambda^2_{L,\mu m}}}, \tag{8}$$

where $I_{L,16}$ is the laser intensity in units of 10^{16} W/cm^{-2}, $\lambda_{L,\mu m}$ is the laser wavelength in microns, and $T_{e,keV}$ is the electron temperature in keV. For parameters in our experiments, Eq. (8) gives $L_{SF} \approx 50$ μm. In inhomogeneous plasma, we can estimate the laser beam radius at the distance z according to the following formula (Andreev & Platonov, 2004)

$$\frac{R}{R_L} \approx 1 - \frac{L_n^2}{L_n^2 + rR_L^2} \frac{z^2}{L_{SF}^2}. \tag{9}$$

For $L_n = 60$ μm and $z = L_{SF}$, one obtain $R \sim 0.3R_L$. Hence, the laser beam radius will decrease approximately by a factor of three and the intensity can increase to the order of magnitude. Such a simple consideration agrees well with the pinhole observation of the laser beam SF (see Figs. 1b and 2).

The ponderomotive laser light pressure squeezes out a portion of electrons from the plasma layer near the critical density area. This effect creates an electric field that accelerates ions. As a result, ions are accelerated in two directions: forward to the laser beam and backward from the target. The energy of these groups of ions can be estimated by the following formulas (Andreev *et al.*, 2002)

$$E_c = \frac{Mv_c^2}{2} \approx \frac{Zm_e c^2 N_c}{N_i}(\gamma - 1),$$
$$E_p = \frac{Mv_p^2}{2} \approx \frac{Zm_e c^2 N_{e,h}}{N_c}(\gamma - 1). \tag{10}$$

Here $\gamma = (1 - a^2)^{1/2}$, $a = v_E/c = 0.8(I_{L,18})^{1/2}$, $I_{L,18}$ is the laser intensity in units 10^{18} W/cm^{-2}, v_p is the speed of an extending plasma boundary, v_c is the speed of the critical surface, $N_{e,h}$ is the density of hot electrons escaping to a vacuum, and N_i is the ion density. For $Z = 7$, $N_c = ZN_i$ and the value of intensity in the experiment $I_L = 4 \times 10^{16}$ W/cm^2 Eq. (10) estimate the energy value 70 keV, and for $a \approx 0.5$, the energy raises up to 500 keV. Note that the transverse velocity of ions due to ponderomotive pressure $v_i/c \approx ct_L/(ZR_L)a^2/\gamma$ (Feit *et al.*, 1996) is small in our conditions and can be neglected.

The expansion of ions in a vacuum is defined also by the ambipolar mechanism (Gurevich *et al.*, 1966). The expression for estimation of the maximal energy of fast ions from Mora (2003) is

$$E_{i,max} \approx 2ZE_{e,h}[\ln(2\omega_{p,i}t_{ef})]^2, \tag{11}$$

where $\omega_{p,i} = (4\pi Z^2 e^2 N_{e,h}/M)^{1/2}$ is the ionic plasma frequency, $t_{ef} \approx 1.5t_L$ (Oishi *et al.*, 2005). The average energy of hot electrons is defined by expression $E_{e,h} \approx 30(10I_{L,18}\lambda^2_{\mu m})^{1/3}T_c^{1/3}$ at rather low laser intensity (Estabrook & Kruer, 1977), and by $E_{e,h} \approx mc^2(\gamma - 1)$ at high intensities (Wilks *et al.*, 2001). For $I_L = 4 \times 10^{16}$ Wcm^{-2}, a similar value $E_{e,h} \approx 10$ keV follows from both formulas. There should be a lack of ions with the energy exceeding $E_{i,max}$ and the distribution function breaks sharply. Eq. (11) for $Z = 7$ and 60 fs pulse duration gives an estimation 100 keV, while for 600 fs duration the energy raises up to 500 keV. These estimations are in good agreement with experimental data as follows from Figure 6.

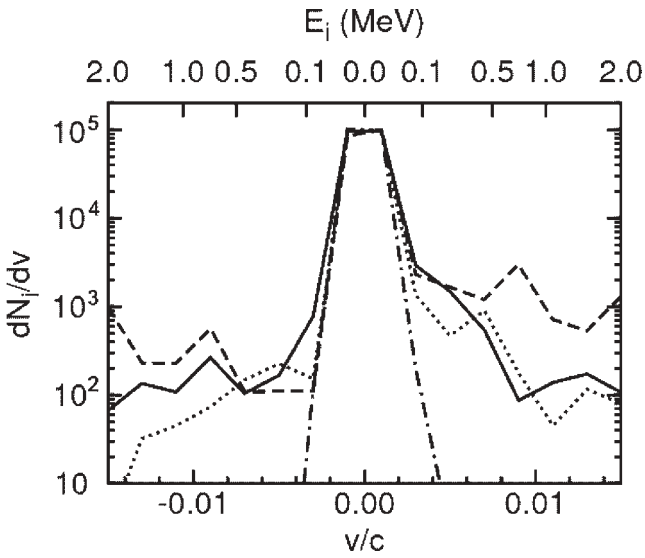

Fig. 7. One-dimensional LPIC kinetic simulation of the ion velocity distribution function in plasma (see text for details) at different laser pulse intensities $I_L = 4 \times 10^{16}$ Wcm^{-2} (dash-dotted curve), 4×10^{17} Wcm^{-2} (dotted curve), and 4×10^{18} Wcm^{-2} (dashed curve) at the middle of the 600-fs laser pulse (solid curves). The solid curve is obtained for $I_L = 4 \times 10^{18}$ Wcm^{-2} and 60-fs laser pulse at the same (300 fs) time moment.

https://doi.org/10.1017/S0263034607000110 Published online by Cambridge University Press

Table 1. *The effective temperatures in the model three-temperature distribution Eq. (3) of the H-like and He-like F ions in plasma produced in the 80-μm foil and slab Teflon targets by the laser pulse with energy $E_L = 128$ mJ and duration $t_L = 1$ ps. The laser intensity in the focal plane at 0.2 mm from a target surface is $I_L \approx 6 \times 10^{16}$ Wcm^{-2}. The electron temperature values are obtained by modeling of the measured He_β and Ly_α line intensities at the electronic density $N_e = 2 \times 10^{20}$ cm^{-3}*

		He_β					Ly_α				
		T_c (keV)	T_w (keV)		T_f (keV)		T_c (keV)	T_w (keV)		T_f (keV)	
CF_2 target	T_e (eV)		Blue	Red	Blue	Red		Blue	Red	Blue	Red
80-μm foil	119	22	80	100	800	1500	6	25	35	700	1400
Slab	122	14	60	90	400	800	5	25	35	250	400

In order to prove these estimations, we have made calculations by the one-dimensional kinetic code linear particle in cells (LPIC). In these calculations, the plasma density had exponentially growing profile of 20 μm in length and the maximal density $5N_c$. It was followed by the 5-μm constant density segment down to the border of calculation area. As the code is one-dimensional, SF was simulated artificially by increasing the laser intensity by an order of magnitude. The results of calculations are shown in Figure 7.

It is clearly seen that at low intensity ($I_L \sim 4 \times 10^{16}$ W cm^{-2}) ions move in forward and backward directions of a laser beam with approximately equal velocities. For higher intensity ions moving forward, have greater velocity and their quantity increases. It agrees well for both with estimations (10) and with the experimental data presented in Figures 5, 6, and in Table 1. From Table 1 follows that the maximal energy of fast ions is higher for the foil target compared to the slab one. The two possible reasons are: re-circulation of very fast electrons in a foil (Sentoku *et al.*, 2003) and generation of another group of fast ions from the foil rear (Wilks *et al.*, 2001). Our calculations show that fast ions have approximately two- or three-temperature distribution function with the temperature values corresponding to experimental data.

4. CONCLUSION

We have measured with high resolution the X-ray spectra of H-like and He-like F ions in plasma produced by low-contrast Ti:Sa subpicosecond laser pulses on the solid Teflon targets as a function of laser pulse energy and duration. From the He_β and Ly_α spectral line shapes, we restore by modeling the ions velocity distribution functions that reveal a generation of fast ions with energy $E \sim 1$ MeV at rather low pulse intensity $I_L \approx 6 \times 10^{16}$ Wcm^{-2} (parameter $F \approx 4 \times 10^{16}$ Wcm^{-2}/μm^2) in a vacuum. The ion distribution functions are anisotropic in the direction of laser beam propagation with an excess of ions moving toward the target. We explain the effect as the result of the laser beam SF in preplasma, created by a big laser prepulse. Laser beam SF essentially increases the local laser intensity in plasma and promotes a fast particle generation, a result confirmed by the numerical kinetic calculation in one-dimensional LPIC simulations. The SF is proved in the measured X-ray pinhole images by the X-ray intensity modulation and laser light channeling along the expanding plasma.

ACKNOWLEDGEMENTS

This work was partly supported by the Russian Foundation for Basic Researches (Projects No. 06-02-16174, 06-02-72005 -МНТИ_а) and by the RAS Presidium Program of basic researches No. 9. The work of A.Y.F. was partly supported by the Landau Network/Cariplo Foundation Fellowship.

REFERENCES

Andreev, A.A. & Platonov, K.Yu. (2004). *Nonlinear optics*. St. Peters: St. Petersburg State University

Andreev, A.A., Limpuch, J., Iskakav, A.B. & Nakano, H. (2002). Enhancement of X-ray line emission from plasmas produced by short high-intensity laser double pulses. *Phys. Rev. E* **65**, 026403.

Andreev, A.A., Platonov, K.Yu., Komarov, V.M., Charukchev, A.V. & Lirtvinenko, I.M. (2002). Generation of a fast-ion beam upon the interaction of a multiterawatt picosecond laser pulse with a solid target. *JETP* **94**, 222.

Auguste, T., Faenov, A.Ya., Fukumoto, I., Hulin, S., Magunov, A.I., Monot, P., D'Oliveira, P., Pikuz, T.A., Sasaki, A., Sharkov, B.Yu., Skobelev, I.Yu., Tajima, T. & Zhidkov, A.G. (2001). Observation of MeV multicharged ions and hot electrons accelerated by a 65-fs laser pulse. *JQSRT* **71**, 147.

Belyaev, V.S., Vinogradov, V.I., Kurilov, A.S., Matafonov, A.P., Andrianov, V.P., Ignatiev, G.N., Faenov, A.Ya., Pikuz, T.A., Skobelev, I.Yu., Magunov, A.I., Pikuz Jr. S.A. & Sharkov, B.Yu. (2004). Neutron production in a picosecond laser plasma for a radiation intensity of 3×10^{17} W/cm^2. *JETP* **98**, 1133.

Belyaev, V.S., Vinogradov, V.I., Matafonov, A.P., Krainov, V.P., Lisitsa, V.S., Faenov, A.Ya., Pikuz, T.A., Skobelev, I.Yu., Magunov, A.I., Pikuz Jr. S.A., Andrianov, V.P., Ignat'ev, G.N., Kozhynov, Yu.I., Kozlov, O.B. & Chekmarev, A.M. (2005). Effective temperature and direction of motion of fast ions in laser produced picosecond plasma. *JETP Lett.* **81**, 753.

Brambrink, E., Roth, M., Blazevic, A. & Schlegel, T. (2006*b*). Modeling of the electrostatic sheath shape on the rear target

https://doi.org/10.1017/S0263034607000110 Published online by Cambridge University Press

surface in short-pulse laser-driven proton acceleration. *Laser Part. Beams* **24**, 163–168.

Brambrink, E., Schreiber, J., Schlegel, T., Audebert, P., Cobble, J., Fuchs, J., Hegelich, M. & Roth, M. (2006*a*). Transverse characteristics of short-pulse laser-produced ion beams: a study of the acceleration dynamics. *Phys. Rev. Lett*. **96**, 154801.

Bulanov, S.V., Pegorato, F. & Pukhov, A. (1995). Two-dimensional regimes of self-focusing, wake field generation, and induced focusing of a short intense laser pulse in an underdense plasma. *Phys. Rev. Lett*. **74**, 710.

Cowan, T.E., Fuchs, J., Ruhl, H., Kemp, A., Audebert, P., Roth, M., Stephens, R., Barton, I., Blazevic, A., Brambrink, E., Cobble, J., Fernández, J., Gauthier, J.-C., Geissel, M., Hegelich, M., Kaae, J., Karsch, S., Le Sage, G.P., Letzring, S., Manclossi, M., Meyroneinc, S., Newkirk, A., Pépin, H. & Renard-LeGalloudec, N. (2004). Ultralow emittance, multi-Mev proton beams from a laser virtual-cathode plasma accelerator. *Phys. Rev. Lett*. **92**, 204801.

Dobosz, S., Schmidt, M., Pedrix, M., Meynadier, P., Gobert, O., Normand, D., Ellert, K., Blenski, T., Faenov, A.Ya., Pikuz, T.A., Skobelev, I.Yu., Magunov, A.I. & Andreev, N.E. (1999). Observation of ions with energy above 100 keV produced by the interaction of a 60-fs laser pulse with clusters. *JETP* **88**, 1122.

Estabrook, K. & Kruer, W. (1977). Properties of resonantly heated electron distributions. *Phys. Rev. Lett*. **40**, 42.

Faenov, A.Ya., Pikuz, S.A., Erko, A.I., Bryunetkin, B.A., Dyakin, V.M., Ivanenkov, G.V., Mingaleev, A.R., Pikuz, T.A., Romanova, V.M. & Shelkovenko, T.A. (1994). High-performance X-ray spectroscopic devices for plasma microsources investigations. *Phys. Scripta* **50**, 333.

Feit, M., Garrison, J.C. & Rubenchik, A.M. (1996). Short pulse laser propagation in underdense plasmas. *Phys. Rev. E* **53**, 1068.

Fernandez, J.C., Hegelich, B.M., Cobble, J.A., Flippo, K.A., Letzring, S.A., Johnson, R.P., Gautier, D.C., Shimada, T., Kyrala, G.A., Wang, Y.Q., Wetteland, C.J. & Schreiber, J. (2005). Laser-ablation treatment of short-pulse laser targets: Toward an experimental program on energetic-ion interactions with dense plasmas. *Laser Part. Beams* **23**, 267–273.

Fuchs, J., Sentoku, Y., Karsch, D., Cobble, J., Audebert, P., Kemp, A., Nikroo, A., Antici, P., Brambrink, E., Blazevic, A., Campbell, E.M., Fernandez, J.C., Gauthier, J.-C., Geissel, M., Hegelich, M., Pepin, H., Popescu, H., Renard-LeGalloudec, N., Roth, M., Schreiber, J., Stephens, R. & Cowan, T.E. (2005). Comparison of laser ion acceleration from the front and rear surfaces of thin foils. *Phys. Rev. Lett*. **94**, 045004.

Fukuda, Y., Akahane, Y., Aoyama, M., Inoue, N., Ueda, H., Kishimoto, Y., Yamakawa, K., Faenov, A.Ya., Magunov, A.I., Pikuz, T.A., Skobelev, I.Yu., Abdallah, J., Jr., Csanak, G., Boldarev, A.S. & Gasilov, V.A. (2004). Generation of X-rays and energetic ions from micron-sized Ar clusters irradiated by ultrafast, high intensity laser pulses. *Laser Part. Beams* **22**, 215.

Gitomer, S.J., Jones, R.D., Begay, F., Ehler, A.W., Kerhart, J.F. & Kristal, R. (1986). Fast ions and hot electrons in the laser–plasma interaction. *Phys. Fluids* **29**, 2679–2688.

Gurevich, A.V., Pariiskaya, L.V. & Pitaevskii, L.P. (1966). Self-similar motion of rarefied plasma. *Sov. Phys. JETP* **22**, 449.

Hegelich, B.M., Albright, B.J., Cobble, J., Flippo, K., Letzring, S., Paffett, M., Ruhl, H., Schreiber, J., Schulze, R.K. & Fernandez, J.C. (2006). Laser acceleration of quasi-monoenergetic MeV ion beams. *Nature* **439**, 441.

Key, M.H., Cable, M.D., Cowan, T.E., *et al*. (1998). Hot electron production and heating by hot electrons in fast ignitor research. *Phys. Plasmas* **5**, 1966–1972.

Kim, K.Y., Milchberg, H., Faenov, A.Ya., Magunov, A.I., Pikuz, T.A. & Skobelev, I.Yu. (2006). X-Ray spectroscopy of 1 cm plasma channels produced by self-guided pulse propagation in elongated cluster jets. *Phys. Rev. E* **73**, 066403.

Kodama, R., Takahashi, K., Tanaka, K.A. *et al*. (1996). Study of Laser-Hole Boring into Overdense Plasmas. *Phys. Rev. Lett*. **77**, 4906.

Krushelnick, K., Clark, E.L., Zepf, M., *et al*. (2000). Energetic proton production from relativistic laser interaction with high density plasmas. *Phys. Plasmas* **7**, 2055–2061.

Laska, L., Jungwirth, K., Krasa, J., Krousky, E., Pfeifer, M., Rohlena, K., Ullschmied, J., Badziak, J., Parys, P., Wolowski, J., Gammino, S., Torrisi, L. & Boody, F.P. (2006). Self-focusing in processes of laser generation of highly-charged and high-energy heavy ions. *Laser Part. Beams* **24**, 175–179.

Lifschitz, A.F., Faure, J., Glinec, Y., Malka, V. & Mora, P. (2006). Proposed scheme for compact GeV laser plasma accelerator. *Laser Part. Beams* **24**, 255–259.

Lindau, F., Lundh, O., Persson, A., *et al*. (2005). Laser-accelerated protons with energy-dependent beam direction. *Phys. Rev. Lett*. **95**, 175002.

Magunov, A.I., Faenov, A.Ya., Skobelev, I.Yu., Pikuz, T.A., Dobosz, S., Schmidt, M., Perdrix, M., Meynadier, P., Gobert, O., Normand, D., Stenz, C., Bagnoud, V., Blasco, F., Roche, J.R., Salin, F. & Sharkov, B.Yu. (2003). X-ray spectra of fast ions generated from clusters by ultrashort laser pulses. *Laser Part. Beams* **21**, 73–79.

Maksimchuk, A., Flippo, K., Krause, H., *et al*. (2004). High-energy ion generation by short laser pulses. *Plasma Phys. Rept.* **30**, 473.

Maksimchuk, A., Gu, S., Flippo, K., *et al*. (2000). Forward ion acceleration in thin films driven by a high-intensity laser. *Phys. Rev. Lett*. **84**, 4108.

Mangles, S.P.D., Walton, B.R., Najmudin, Z., Dangor, A.E., Krushelnick, K., Malka, V., Manclossi, M., Lopes, N., Carias, C., Mendes, G. & Dorchies, F. (2006). Table-top laser-plasma acceleration as an electron radiography source. *Laser Part. Beams* **24**, 185–190.

Mora, P. (2003). Plasma expansion into a vacuum. *Phys. Rev. Lett*. **90**, 185002.

Mourou, G.A., Tajima, T. & Bulanov, S.V. (2006). Optics in the relativistic regime. *Rev. Mod. Phys*. **78**, 309.

Oishi, Y., Andreev, A., *et al*. (2005). Dependence on laser intensity and pulse duration in proton acceleration by irradiation of ultra-short laser pulse on a Cu foil target. *Phys. Plasmas* **12**, 073102.

Rosmej, F.B., Stepanov, A.E., Hoffmann, D.H.H., Faenov, A.Ya., Suss, W., Geissel, M., Pirzadeh, P., Seelig, W., Skobelev, I.Yu., Magunov, A.I., Pikuz, T.A., Bock, R., Letardi, T., Flora, F., Bollanti, S., Di Lazzaro, P., Satov, Yu.A., Smakovskii, Yu.B., Roerich, V.K., Khomenko, S.V., Makarov, K.N., Starostin, A.N., Reale, A., Scafati, A., Auguste, T., D'Oliveira, P., Hulin, S., Monot, P. & Sharkov, B.Yu. (2002). The generation of fast particles in plasmas created by laser pulses with different wavelengths. *JETP* **94**, 60.

Rosmej, O.N., Pikuz, S.A., Korostiy, S., Blazevic, A., Brambrink, E., Fertman, A., Mutin, T., Efremov, V.P., Pikuz, T.A., Faenov, A.Y., Loboda, P., Golubev, A.A. & Hoffmann, D.H.H. (2005).

Radiation dynamics of fast heavy ions interacting with matter. *Laser Part. Beams* **23**, 79–85.

Schaumann, G., Schollmeier, M.S., Rodriguez-Prieto, G., Blazevic, A., Brambrink, E., Geissel, M., Korostiy, S., Pirzadeh, P., Roth, M., Rosmej, F.B., Faenov, A.Y., Pikuz, T.A., Tsigutkin, K., Maron, Y., Tahir, N.A. & Hoffmann, D.H.H. (2005). High energy heavy ion jets emerging from laser plasma generated by long pulse laser beams from the NHELIX laser system at GSI. *Laser Part. Beams* **23**, 503–512.

Sentoku, Y., Cowan, T., Kemp, A. & Ruhl, H. (2003). High energy proton acceleration in interaction of short laser pulse with dense plasma target. *Phys. Plasmas* **10**, 2009–2015.

Skobelev, I.Yu., Faenov, A.Ya., Bryunetkin, B.A., Dyakin, V.M., Pikuz, T.A., Pikuz, S.A., Shelkovenko, T.A. & Romanova, V.M. (1995). Investigations of radiative properties of plasma sources by image X-ray spectroscopic methods. *JETP* **81**, 692.

Sun, G.-Zh., Ott, E., Lee, Y.C. & Guzdar, P. (1987). Self-focusing of short intense pulses in plasmas. *Phys. Fluids* **30**, 526–532.

Tighe, R.J. & Hooper Jr. C.F. (1976). Stark broadening in hot, dense laser-produced plasmas. *Phys. Rev. A* **14**, 1514.

Wilks, S.C., Langdon, A.B., Cowan, T.E., *et al*. (2001). Energetic proton generation in ultra-intense laser–solid interactions. *Phys. Plasmas* **8**, 542–549.

Yin, L., Albright, B.J., Hegelich, B.M. & Fernandez, J.C. (2006). GeV laser ion acceleration from ultrathin targets: The laser break-out afterburner. *Laser Part. Beams* **24**, 291–298.

Zhidkov, A.G., Sasaki, A., Fukumoto, I., Tajima, T., Auguste, T., D'Olivera, P., Hulin, S., Monot, P., Faenov, A.Ya., Pikuz, T.A. & Skobelev, I.Yu. (2001). Transient distribution of energetic particles produced by intense femtosecond laser pulses irradiating solids. *Phys. Plasma* **8**, 3718.

Zhidkov, A.G., Sasaki, A., Tajima, T., Auguste, T., D'Oliveira, P., Hulin, S., Monot, P., Faenov, A.Ya., Pikuz, T.A. & Skobelev, I.Yu. (1999). Direct spectroscopic observation of multiple charged ion acceleration by intense femtosecond pulse laser. *Phys. Rev. E* **60**, 3273.

https://doi.org/10.1017/S0263034607000110 Published online by Cambridge University Press